ELSEVIER

Contents lists available at ScienceDirect

Applied Acoustics

journal homepage: www.elsevier.com/locate/apacoust



Road profile estimation using the dynamic responses of the full vehicle model



Dorra Ben Hassen^a, Mariem Miladi^a, Mohamed Slim Abbes^a, S. Caglar Baslamisli^b, Fakher Chaari^{a,*}, Mohamed Haddar^a

- a Mechanics, Modelling and Production Laboratory (LA2MP), National Engineering School of Sfax (ENIS), BP 1173, 3038 Sfax, Tunisia
- ^b Hacettepe University, Dept. of Mechanical Eng. 06800 Beytepe, Ankara, Turkey

ARTICLE INFO

Keywords: Road profile Full car model Quarter car Pitch model Roll model Independent Component Analysis Robustness

ABSTRACT

The purpose of this paper was to estimate the road profile irregularities that affect vehicles. The studied random road profiles are related to the ISO 8608 standard. The identification of these disturbances is very important to select the adequate control law for an active suspension. Many studies have been carried out in this field but they were either costly because their road profile measurements were achieved using longitudinal profile analyser or laser sensors or needed long computation time particularly the neural network based models. This study proposed the implementation of a new fast and simple technique, called the Independent Component Analysis (ICA) to identify the road profile, based on the so-called inverse problem. Knowing the dynamic responses of the system (observed signals), the ICA allows the identification of road excitation. These responses can be either measured via sensors or computed numerically. To this end, three models were studied: a full car model, a half car (pitch-bounce and roll model) and a quarter car. The full car is considered as the real model. So the dynamic responses, which make up the ICA observed signals, are computed from this model. In the second part of this paper, we studied the ICA efficiency to construct the estimated road profile. The obtained results were validated using some performance criteria and the robustness of the method was assessed using the sprung mass variation and noise effect. The obtained results show that the ICA can identify the road disturbances adequately.

1. Introduction

The knowledge of the different excitations applied to a vehicle has been the objective of many studies for decades. Since the vehicle performance is affected by the road disturbances [1], such as the ride quality and the road holding [2], pushing the researches to the choice of adequate control laws, many authors have turned to focus on the identification of these disturbances. Some of them proposed direct measurements of the profile [3] or information acquisition from sensors installed on a vehicle [4,5]. These methods are however very expensive [3]. Others were interested in using the Neural Network models, which were reveled to be very complicated and needed a long computation time [3]. Another group focused on the use of the estimation methods based on Monte Carlo algorithm such as Harris et al. [6], while some authors relied on the Kalman filter to estimate the road profile [3–7]. This technique is efficient but requires the tuning of the algorithm on the one hand, and it is affected by the load variability applied to the vehicle, on the other. All these techniques remain interesting but they all have their own shortcomings as mentioned above.

For this purpose, this paper aimed to extract the road profile using a new technique called the Independent Component Analysis, which is based on the resolution of the inverse problem. This technique is able to estimate the road profile using only the dynamic responses of the vehicle. The ICA is an efficient method that was used by Akrout et al. [8] to estimate the excitation forces applied on discrete and continuous beam. Also, It was implemented in the Operational Modal Analysis to determine the eignfrequenices and the modal parameters of a given mechanical system [9]. The ICA does not require a long computation time and it is easy to use. It just needs the dynamic responses of the studied system, collected by available and conventional sensors such as accelerometers and the suspension deflections. These sensors provide a good estimation of road profile variability [1–3]. Such advantages make the proposed method simple and cheap enough to be used in real time, since it allows gathering road information when the vehicle is rolling. The obtained results were validated by computing different performance criteria. This would be of great importance to better understand the vehicle dynamics and apply the control laws for active suspensions.

The remainder of this paper was organized as follows: in a second

E-mail address: fakher.chaari@enis.rnu.tn (F. Chaari).

^{*} Corresponding author.

section, the ICA technique was presented and the studied models were detailed together with the simulation results. They were then, validated by some performance criteria and a good agreement between the original signals and the estimated ones was shown. Finally, the robustness of the proposed method was studied varying the sprung mass and showing the noise effect.

2. The independent component analysis

2.1. Motivation

The Independent Component Analysis is based on Blind Source Separation (BSS). This method consists in recovering the original sources knowing only the observed signals, which represent a mixture of these signals. To better understand this definition, the example of the simple 'Cocktail party' problem was illustrated [10].

This problem consists in supposing that there are two people speaking at the same time in the same room and two microphones placed in different locations are recording the time signals noted by $x_1(t)$ and $x_2(t)$. Each of these recorded signals is a mixture of the original signals $s_1(t)$ and $s_2(t)$ emitted by the two speakers. This problem could be expressed as:

$$x_1(t) = a_{11}s_1 + a_{12}s_2 \tag{1}$$

$$x_2(t) = a_{21}s_1 + a_{22}s_2 \tag{2}$$

So the vector of the observed signals X can be written in a matrix form as [11,12]:

$${X} = {A}{S}$$
 (3)

where [A]: the mixing matrix and {S}: the vector of source signals.

The task consists in estimating both [A] and $\{S\}$ relying only on the knowledge of the observed signal $\{X\}$.

2.2. Assumptions

In order to find the estimated sources, The ICA seeks for the directions that are the most independent. This can be achieved taking into account these assumptions [10,11]:

- The component of the vector S must be both statistically independent and have non gaussian distribution.
- The number of the estimated sources is equal to the number of observed signals.

So, the ICA can define each column of the matrix A and then compute the separating matrix [W] as:

$$[W] = [A]^{-1} \tag{4}$$

Then the ICA estimates the corresponding source signal defined by:

$$\{S\} = [W]\{X\} \tag{5}$$

After that, the observed signal $\{X\}$ undergoes some pre-treatments [10–12]. These pre-treatments are centering and whitening. Centering means subtracting its mean vector m=E(X). Therefore, each signal becomes a zero-mean variable so that we obtain a zero mean source signal. As for whitening it means that the measured signal X becomes white signal X with uncorrelated components and a variance equal to the unit [10].

As a whitening method, we can use the eigenvalue decomposition of the covariance matrix:

$$E\{XX^{T}\} = EDE^{T}$$
(6)

where E is the orthogonal matrix of eigenvectors of $E\{XX^T\}$ and D is the diagonal matrix of its eigenvalues. A whitening transform is then given by:

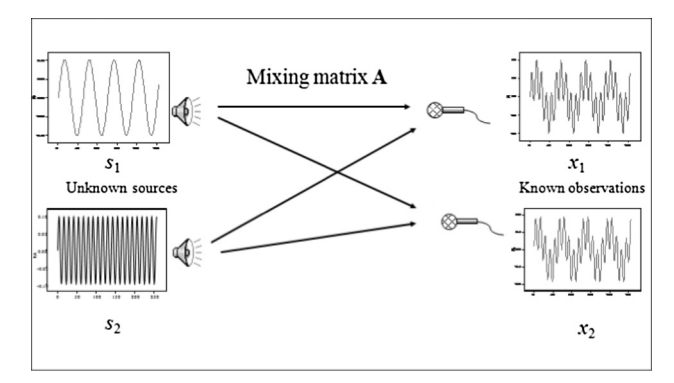


Fig. 1. Cocktail party problem.

$$\widetilde{X} = E D^{-1/2} E^T X \tag{7}$$

So that we are able to determine each column of the separating matrix by the ICA and then the source related to this column is extracted. It is defined by:

$$\{Y\} = [W]^{H}\{X\} \tag{8}$$

where (.)^H denotes the conjugate-transpose operator. It should be noted that [W] must satisfy the criterion of non gaussianity distribution. So it has to maximize the kurtosis defined by Zarzoso and Comen [13] as the normalized fourth-order marginal cumulate defined by the following equation in order to guarantee a non-Gaussianity distribution.

$$K(ka) = \frac{E\{|y|^4\} - 2E^2\{|y^2|\} - |E\{y^2\}|^2}{E^2\{|y^2|\}}$$
(9)

Finally, after the determination of the first column of the matrix [W] the ICA uses the deflation approach to extract the estimated sources. So, each source will be chosen once with multiplying factor. The following figure summarizes the concept of the ICA method (see Figs. 1 and 2).

3. Studied cases

3.1. Full car vehicle model

The studied model of the full vehicle is presented in Fig. 3.

The parameters of this seven-degree freedom model are the following: $m_{\rm ff}$ is the body mass of the vehicle, I_x is a longitudinal mass moment of inertia, and I_y is a lateral mass moment of inertia. The mass of the wheels are expressed respectively by: m_1 , m_2 , m_3 , and m_4 .

 k_f and k_r are the front and rear suspension stiffness. k_{tf} and k_{tr} are the tire stiffness in the front and rear respectively.

 C_f and C_r are the front and rear damping.

The values of these parameters are presented in Appendix A.1.1 This model motion equations are summarized in a matrix form (see Appendix A.1.2)

3.2. Quarter vehicle model

The studied quarter model is presented in Fig. 4. This model can describe the vehicle body bounce vibration mode [14]. However this model does not consider the pitch and roll motions.

Therefore, these two modes will be taken into account by studying the half car model (pitch model and roll model [14]).

This system has two degrees of freedom: x_1 is the displacement of the sprung mass m_s while x_2 is the displacement of unsprung mass m_{us} : The suspension system is modeled as a linear damper in parallel with a linear spring. The parameters of the studied system are presented in Appendix A.2.1 and the motion equations of the studied system are presented in Appendix A.2.2.

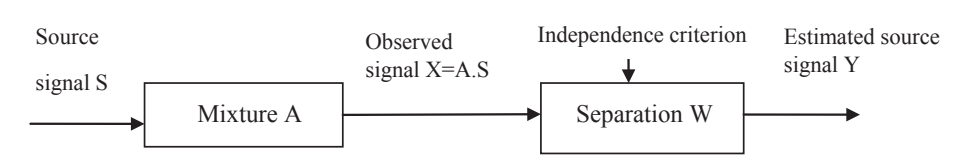
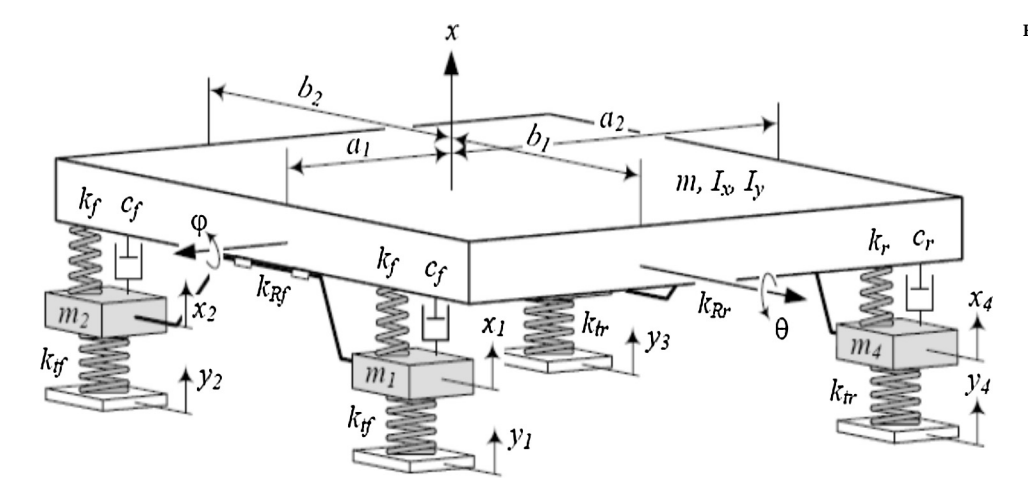


Fig. 2. ICA concept.

Fig. 3. Full car vehicle model [14].



3.3. Half vehicle model (pitch-bounce model)

In order to introduce the pitch motion of the vehicle, the half vehicle model, which includes pitch and other vibration modes, was studied in this section. The pitch bounce model [14] is given in Fig. 5.

This model includes the body bounce x, body pitch θ ; wheels hop x_{p1} and x_{p2} and the road disturbances r_1 and r_2 .

The parameters of the studied system are presented in Appendix A.3.1.

The motion equations can be expressed in a matrix form as shown in Appendix A.3.2

3.4. Half vehicle model (roll model)

This model investigated the roll vibration of the vehicle. It included the body bounce x_b , body roll ϕ ; wheels hop x_{u1} and x_{u2} and the road disturbances h_1 and h_2 . It is presented in Fig. 6.

The motion equations and the parameters of this model are presented respectively in Appendices A.4.1 and A.4.2.

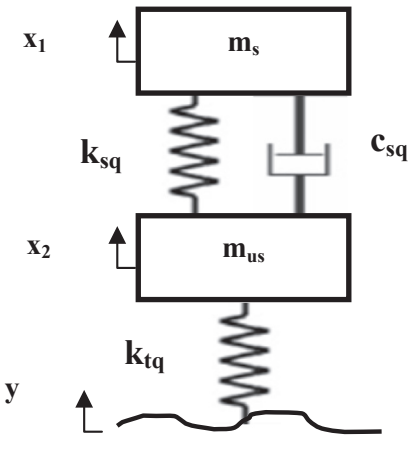


Fig. 4. Quarter car model.

4. Road disturbance

As far as the road disturbances are concerned, a random road profile, which is closest to reality according to ISO 8608 standard, was adopted. The ISO assumes that the roads are classified in five main classes (from A to E) according to their roughness. The random profile was constructed using this equation [2]:

$$\dot{\mathbf{y}}_r(t) + \mathbf{w}_0 \mathbf{y}_r(t) = \sqrt{\mathbf{Sg}(\Omega_0) \cdot \mathbf{v} \cdot \mathbf{w}(t)}$$
(10)

where y_r (t): is the road profile, v: is the car velocity, it is equal to 15 m/s; w (t): is the noise signal and $w_0=0.2~\pi v$; Sg (Ω_0) is the road roughness.

The International Organization for Standardization (ISO) proposed a classification of different road roughness classes (Class A to E) as shown in Table 1. Class A represents a very good road surface which becomes poorer as it goes down to Class E.

For our study it is assumed that generic roads are the real ones. From the influence of these roads on the vehicle, the sensors can measure the dynamic responses of our system, so that the chassis acceleration and the suspension deflection are collected from the full model. These measurements represent the vector of the observed signals for the ICA algorithm. This vector contains the mixing matrix and

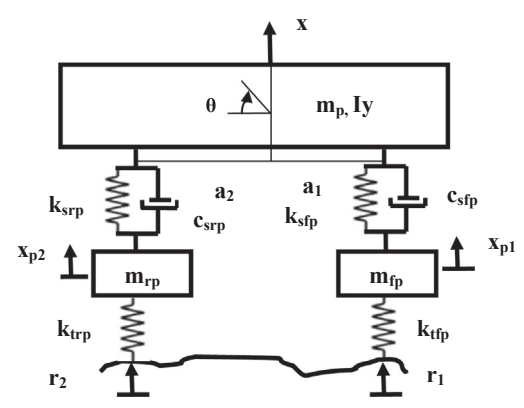


Fig. 5. Half vehicle model (pitch-bounce model).

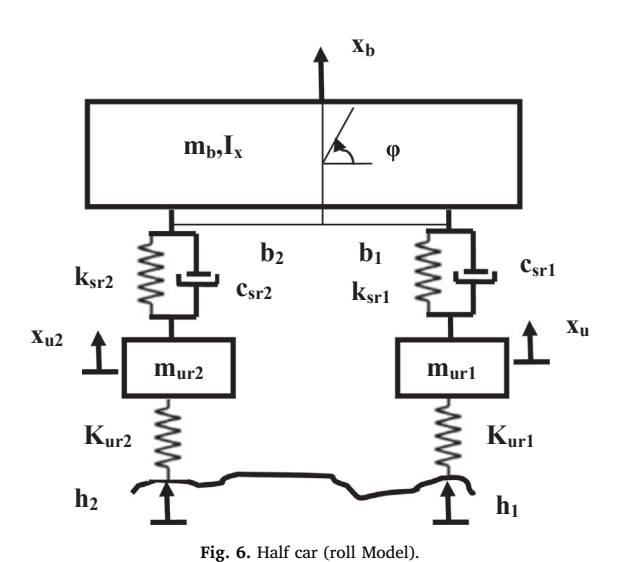


Table 1
Classification of road roughness by ISO.

Road class	Degree of roughness Sg (Ω_0) ($10^{-6}~\text{m}^2/\text{cycle/m}$)		
	Range	Geometric mean	
A (very good)	< 8	4	
B (good)	8-32	16	
C (Average)	32-128	64	
D (poor)	128-512	256	
E (very poor)	512-2048	1024	

the estimated source signals. The ICA uses the permutation of the estimated sources and random profiles that are constructed close to the generic roads in order to extract the exact road profile with a multiplying factor. The estimated profile is then compared with the generic road.

5. Description of the method of the application of the ICA for the identification of the road profile

The ICA is applied in this study on different dynamic models of cars: the quarter car, the half car (pitch-bounce model and roll model). The implementation of this method was based only on the knowledge of the dynamic responses of the system.

In our case, we did not have any experimental measurements so the dynamic responses of the different studied models were computed numerically from the vibratory responses of the full model, considered as a reference model (the closest to real model). These responses were determined using Newmark algorithm under the following excitations:

- Excitation1: Front Right wheel: Random profile from A to E.
- Excitation 2: Front left wheel: Excitation2 using another road profile

Table 2
Natural frequencies (in Hz).

Model Frequency	Full Model	Quarter car	Pitch model	Roll model
F1	0.7		\searrow	0.82
F2	0.95	0.96	1.01	1.01
F3	1.2		1.4	\mathbb{N}
F4	8.25		$\backslash\!$	$\backslash\!\!\!\backslash$
F5	8.3		8.16	\mathbb{N}
F6	9.86	\searrow	\bigvee	9.84
F7	9.92	9.8	9.83	9.88

from A to E.

- Excitation3: Rear left wheel: Excitation2 plus delay
- Excitation 4: Rear right wheel: Excitation1 plus delay.
- For the quarter car model, two measurements were required:
 - Suspension deflection (Δq): equal to the mean of the four suspension deflections of the full model.
- Chassis acceleration (a_c): equal to the chassis acceleration of the full model.
- For the pitch model the dynamic responses were computed as follows:
- Suspension deflection of the front wheels (Δ1p): equal to the mean
 of the suspension deflection of the front wheels of the full car.
- Suspension deflection of the rear wheels (Δ2p): equal to the mean of the suspension deflection of the rear wheels of the full car.
- Chassis acceleration (a_c): equal to the chassis acceleration of the full model.
- For the roll model, the dynamic responses were computed as follows:
 - Suspension deflection of the right wheels (Δ1r): equal to the mean of the suspension deflection of the right wheels of the full car.
 - Suspension deflection of the left wheels ($\Delta 2r$): equal to the mean of the suspension deflection of the left wheels of the full car.
 - Chassis acceleration (a_c): equal to the chassis acceleration of the full model.

These responses were used as input signals for the ICA program: From these responses only, the ICA would identify the road profile for the three studied models.

The following diagram explains further the method.

6. Simulation results

This section was split into two parts: the first presented the frequency response of all the studied models in order to compare their behavior with the real model and confirmed that they were close to each other. The second part detailed the application of the ICA and the obtained results in order to check the best model that could represent a full vehicle.

6.1. Frequency response of the studied systems

The diagram of bode of the vehicle models shows that they were close to the real model in terms of frequencies. The obtained natural frequencies are summarized in Table 2.

Since the frequency responses of the three studied system were close to the real model (full model) frequencies, we presented the time response of the road estimation of the three studied systems in the following section in order to decide about the best one which described the real road profile (see Tables 3 and 4).

6.2. Road profile estimation using the ICA

In this part of the paper, the three studied models were subjected to

Table 3
Simulation time for road A and E estimation.

	Quarter car model	Pitch model	Roll model
Simulation time (s)	Road profile A 0.52	0.7014	0.8019
	Road profile E 0.52	0.55	0.67

Table 4
Performance criteria.

Road profile	Studied models	MAC	$\mathbf{E}_{\mathbf{r}}$	E _f (%)
Road A	Quarter car	0.65	0.01	20.1
	Pitch model (Excitation1)	0.62	0.0116	23
	Pitch model (Excitation2)	0.64	0.0109	15.11
	Roll model (Excitation1)	0.64	0.2	4.5
	Roll model (Excitation2)	0.51	0.15	34.19
Road E	Quarter car	0.61	0.016	7.1
	Pitch model (Excitation1)	0.67	0.010	7.8
	Pitch model (Excitation2)	0.62	0.017	2.71
	Roll model (Excitation1)	0.48	0.010	23.5
	Roll model (Excitation2)	0.49	0.132	29.9

random excitations as described in Section 3.4. The application of the ICA was based on the measured responses to guarantee a good estimation of the road profile variability. The following figures show the comparison between the generic road profile (type A and E as examples) which presented the real road profile signal and the estimated signal of the constructed prototype for the different models. In fact: for the quarter car model the estimated profile is compared with the mean of the four excitations applied on the wheels of the full model. For the pitch model, two excitations are obtained: the Front excitation which is compared with the mean of the two front excitations of the full model and the rear excitation compared with the mean of the two rear excitations applied on the full model. Finally, for the roll model, two excitations are obtained: the right excitation which is compared with the mean of the two right excitations of the full model and the left

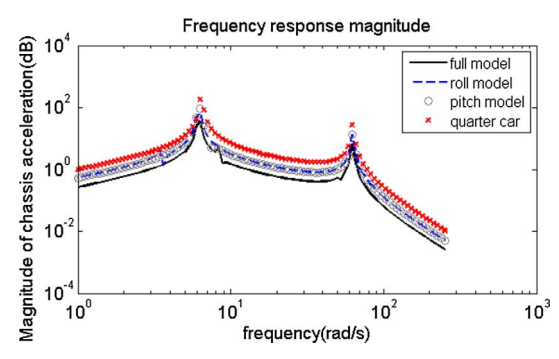


Fig. 8. Bode diagram of the studied systems.

excitation compared with the mean of the two left excitations applied on the full model. Besides, the simulation time for the two types of road profile was displayed (see Figs. 7–10).

It can be noticed that, using the three different models, the ICA can reconstruct the original road profiles (A and E). Also the simulation time was very small and this proved that the ICA is a fast technique that can be used in real time. For the quarter model one excitation was identified and for the two other models, two excitations were identified. To study the efficiency of this method, three performance criteria were investigated [15]:

• The Modal Assurance Criterion is defined as follows: MAC

$$Mac_{i} = \frac{(S_{i}^{T}\overline{S}_{i})^{2}}{(S_{i}^{T}S_{i})(\overline{S}_{i}^{T}\overline{S}_{i})}$$

$$\tag{11}$$

where S_i and \overline{S}_i are respectively the real and the estimated road profiles. If the MAC value is near zero, then the two signals are not conform. But if MAC has a value of about the unit, this is an indication that the two signals are close to each other.

 The Euclidean distance between the two signals in order to calculate the approximation error is calculated as follows:

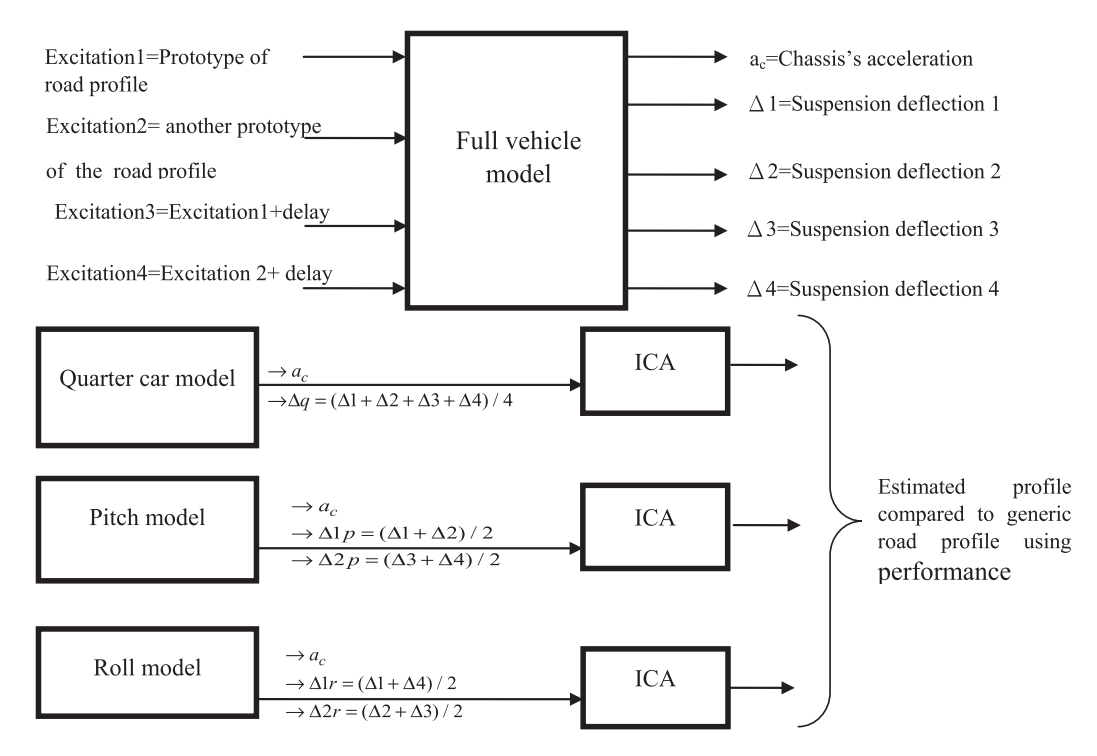
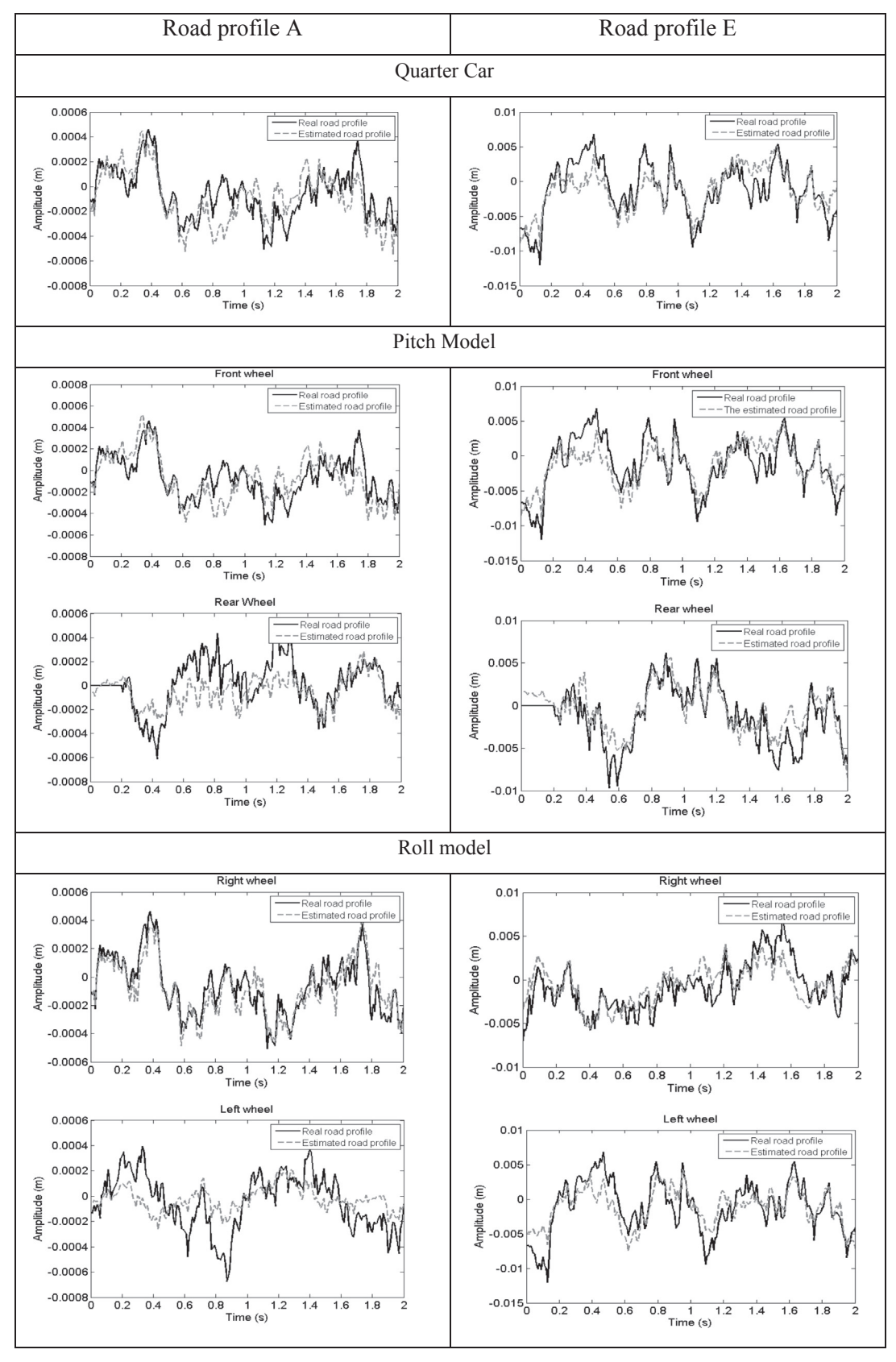


Fig. 7. The method diagram.



 $\textbf{Fig. 9.} \ \ \textbf{Road} \ \ \textbf{A} \ \ \textbf{and} \ \ \textbf{E} \ \ \textbf{estimation} \ \ \textbf{using the different vehicle models}.$

10⁻⁴ Real road profile A (a) Real road profile B PSD Amplitude m/Hz Real road profile C Real road profile D -Real road profile E Estimated road profile A Estimated road profile B Estimated road profile C Estimated road profile D - ← - Estimated road profile E 10 10⁰ 10¹ 10 10 102 Frequency (Hz) 10 Real road profile A (b) Real road profile B PSD Amplitude m/Hz Real road profile C 10⁻⁶ -Real road profile D Real road profile E --Estimated road profile A Estimated road profile B --- Estimated road profile C - = Estimated road profile D ◆ - Estimated road profile E 10-11 10 10-2 10 10⁰ 10 102 Frequency (Hz) 10⁻⁴ Real road profile A (c) -Real road profile B Real road profile C PSD Amplitude m/Hz 10 -Real road profile D -Real road profileE -Estimated road profile A -Estimated road profileB Estimated road profile C Estimated road profile D Estimated road profile E 10 10⁻¹ 10⁰ 10 10 10 Frequency (Hz)

Fig. 10. Comparison of the original profile and the estimated one PSDs using the different models (a) quarter car (b) pitch model (c) roll model.

$$\mathbf{E}_{\mathrm{ri}} = \|\mathbf{S}_{\mathrm{i}} - \overline{\mathbf{S}}_{\mathrm{i}}\| \tag{12}$$

 The relative error E_{fi} between the exact and estimated signal present good performance criteria is defined as follows:

$$E_{fi}(\%) = 100 \frac{|S_i - \overline{S}_i|}{S_i} \tag{13}$$

The following table summarizes the values of the performance criteria of the studied models using the random road A and E.

It can be noticed that the ICA shows satisfactory results for the

estimation of the different road profiles (Mac value is close to one and the relative errors are minimum compared to those obtained by W. Fauriat in Ref. [3]). So this estimation method provides a good description of the generic road variability. To confirm the efficiency of the method and validate the obtained results, the original signals PSDs and the estimated ones were presented.

The comparison of the PSDs allows us to notice that the estimator performs very well for the three studied models.

So, the estimation results using the ICA are sufficient to recover the real profile based on simplified models and there is no need to use complex models to estimate the road profile.

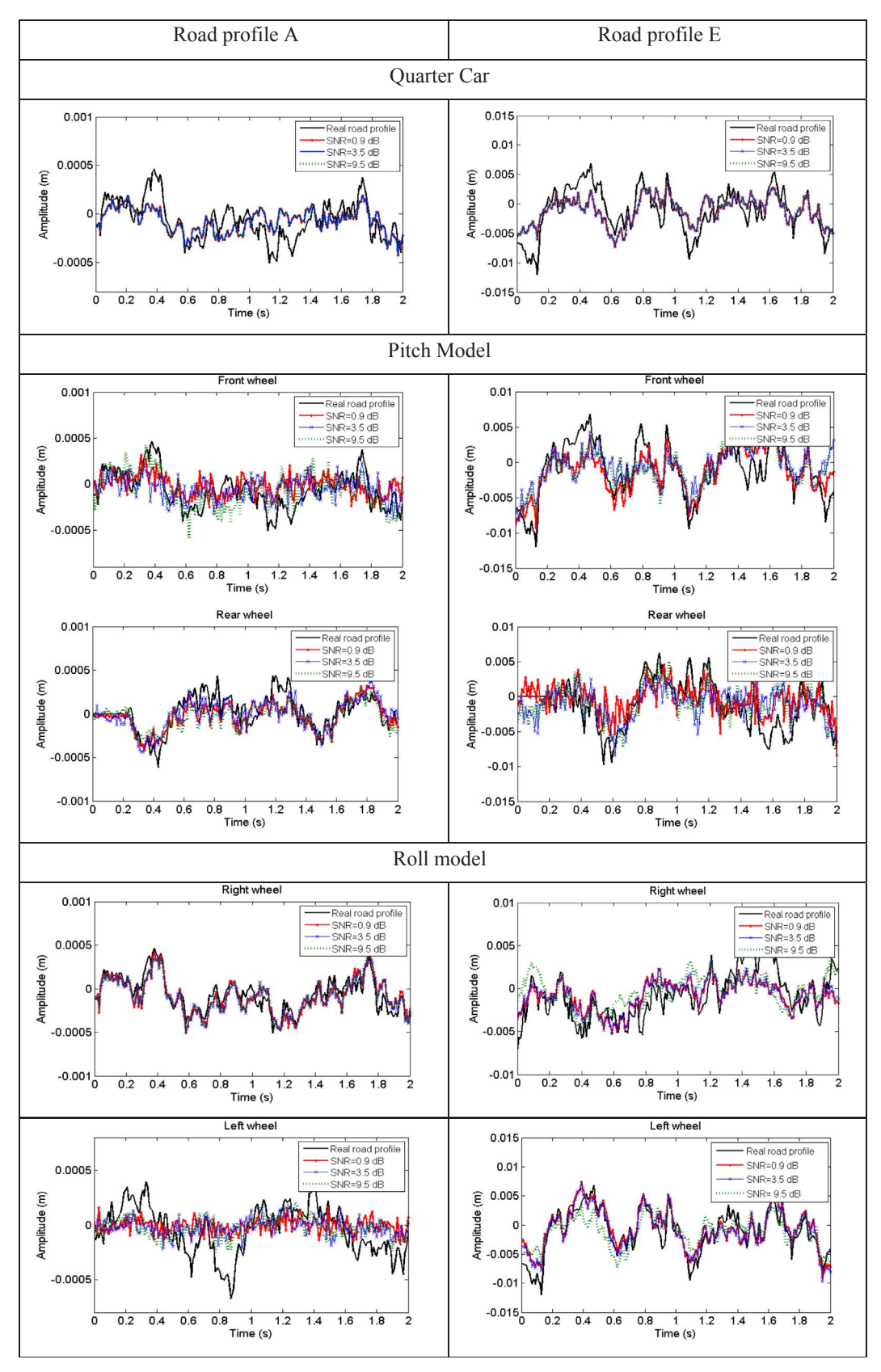


Fig. 11. The noise effect on the estimation process for road profile type A and E.

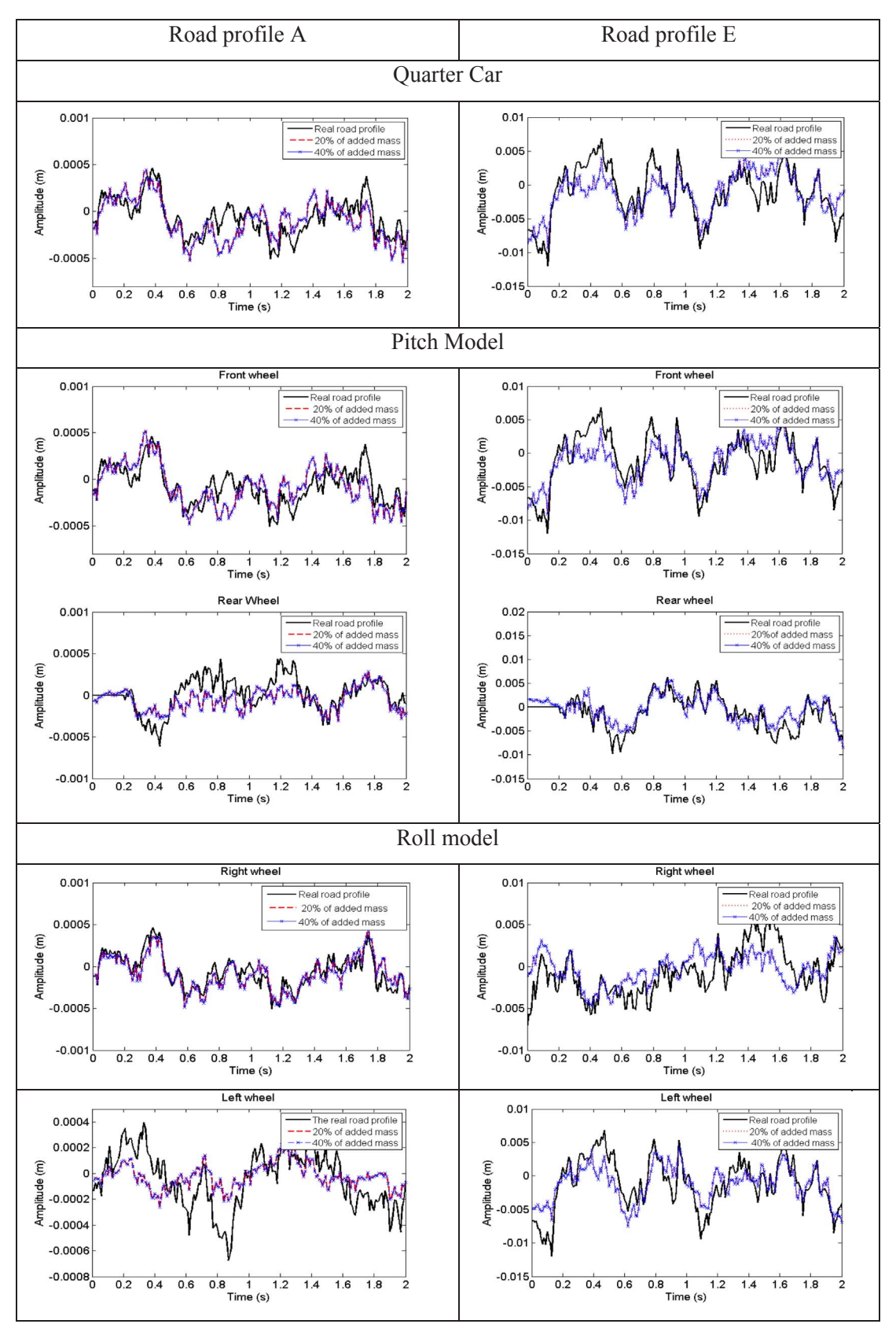


Fig. 12. Effect of the sprung mass variation on the estimation of road profile A and E.

7. Robustness of the method

7.1. Effect of random noise

To check the ability of the ICA method to reconstruct the real road profiles, a random noise with a Gaussian distribution was added to the measured responses. This mixture allows obtaining the disturbed estimated sources for the two roads type A and E presented in Fig. 11. The simulations were run for signal-to-noise ratio (SNR) between 0.9 dB and 9.5 dB for the two types of road profiles. The three runs displayed are as shown in the figure below.

When comparing the road profile without noise and those with additional noise, it is clearly noticeable that the ICA can well estimate the profiles even with a high level of noise for the two studied types of road profiles.

7.2. Effect of sprung mass variation

Since any vehicle has a major activity which is the transport of people or items, we proposed to study the efficiency of the ICA via the sprung mass variation in this sub section. So we assumed that the additional payload was applied on the sprung mass by a range of 20% and 40% as shown in Fig. 12.

Appendix A

A.1. Full car model

A.1.1. Full car model parameters

See Table A1.

Table A1 the parameters of the full car model [14].

Even with increasing the value of the sprung mass by a range of 40%, the ICA remains able to estimate the two types of road profiles through the three studied models.

8. Conclusion

In this paper, the ICA was implemented to three different models of a vehicle: Half car (pitch-bounce and roll) and quarter car. This technique was used to estimate the road disturbance knowing only the dynamic responses of the full vehicle model. Compared to all the other estimation techniques, the ICA is simpler, faster and requires available sensors, which are the chassis acceleration and the suspension deflection. By the computation of the different performance criteria between the original signals and the estimated ones, it can noticed that the three studied models give a good estimation of the road profile. Also, the ICA is robust to the sprung mass variation and the addition of noise has a small effect on the estimation process.

Thus, there is no need to use a more complex full car model in order to estimate the road profile. This will be very interesting when designing control law for active suspension in a future work. Therefore, as a perspective we are planning to validate the ICA technique experimentally.

Parameters	Value	Variable unit
Mass of the chassis	m _{ff} = 840	[kg]
Mass of the front tire	$m_{\rm f} = 53$	[kg]
Mass of the rear tire	$m_{\rm r} = 76$	[kg]
Roll moment of inertia	$I_x = 820$	[kg/m ²]
Pitch moment of inertia	$I_v = 1100$	[kg/m ²]
Distance of gravity centre from front axle	$a_1 = 1.4$	[m]
Distance of gravity centre from rear axle	$a_2 = 1.47$	[m]
Distance of gravity centre from right axle	$b_1 = 0.7$	[m]
Distance of gravity centre from left axle	$b_2 = 0.75$	[m]
Stiffness of the front suspension	$k_f = 10,000$	[N/m]
Stiffness of the rear suspension	$k_r = 13,000$	[N/m]
Stiffness of the tire	$k_{tf} = k_{tr} = 20 \cdot 10^4$	[N/m]
Damping coefficient	$c_f = c_r = 1000$	[N/ms]

A.1.2. Full car model equations of motion

$$M = \begin{bmatrix} m_{ff} & 0 & 0 & 0 & 0 & 0 & 0 \\ 0 & I_X & 0 & 0 & 0 & 0 & 0 \\ 0 & 0 & I_Y & 0 & 0 & 0 & 0 \\ 0 & 0 & 0 & m_f & 0 & 0 & 0 \\ 0 & 0 & 0 & 0 & m_f & 0 & 0 \\ 0 & 0 & 0 & 0 & 0 & m_r & 0 \\ 0 & 0 & 0 & 0 & 0 & 0 & m_r \end{bmatrix}$$

$$K = \begin{bmatrix} k_{11} & k_{12} & k_{13} & -k_f & -k_f & -k_r & -k_r \\ k_{21} & k_{22} & k_{23} & k_{24} & k_{25} & b_1k_r & -b_2k_r \\ k_{31} & k_{32} & k_{33} & a_1k_f & a_1k_f & -a_2k_r & -a_2k_r \\ -k_f & k_{42} & a_1k_f & k_{44} & 0 & 0 & 0 \\ -k_f & k_{52} & a_1k_f & 0 & k_{55} & 0 & 0 \\ -k_r & b_1k_r & -a_2k_r & 0 & 0 & k_f + k_{tr} & 0 \\ -k_r & -b_2k_r & -a_2k_r & 0 & 0 & 0 & k_r + k_{tr} \end{bmatrix}$$

$$C = \begin{bmatrix} c_{11} & c_{12} & c_{13} & -c_f & -c_f & -c_r & -c_r \\ c_{21} & c_{22} & c_{23} & -b_1c_f & b_2c_f & b_1c_r & -b_2c_r \\ c_{31} & c_{32} & c_{33} & a_1c_f & a_1c_f & -a_2c_r & -a_2c_r \\ -c_f & -b_1c_f & a_1c_f & c_f & 0 & 0 & 0 \\ -c_f & b_2c_f & a_1c_f & 0 & c_f & 0 & 0 \\ -c_r & b_1c_r & -a_2c_r & 0 & 0 & c_r & 0 \\ -c_r & -b_2c_r & -a_2c_r & 0 & 0 & 0 & c_r \end{bmatrix} \quad F = \begin{bmatrix} 0 \\ 0 \\ 0 \\ y_1k_{tf} \\ y_2k_{tf} \\ y_3k_{tr} \\ y_4k_{tr} \end{bmatrix}$$

where

$$c_{11} = 2c_f + 2c_r$$

$$c_{12} = c_{21} = b_1 c_f {-} b_2 c_f {-} b_1 c_r \, + \, b_2 c_r$$

$$c_{31} = c_{13} = 2a_2c_r - 2a_1c_f$$

$$c_{22} = b_1^2 c_f + b_2^2 c_f + b_1^2 c_r + b_2^2 c_r$$

$$c_{32} = c_{23} = a_1b_2c_f - a_1b_1c_f - a_2b_1c_r + a_2b_2c_r$$

$$c_{33} = 2c_f a_1^2 + 2c_r a_2^2$$

$$k_{11} = 2k_f + 2k_r$$

$$k_{12} = k_{21} = b_1 k_f - b_2 k_f - b_1 k_r + b_2 k_r$$

$$k_{31} = k_{13} = 2a_2k_r - 2a_1k_f$$

$$k_{22} = b_1^2 k_f + b_2^2 k_f + b_1^2 k_r + b_2^2 k_r$$

$$k_{32} = k_{23} = a_1 b_2 k_f - a_1 b_1 k_f - a_2 b_1 k_r + a_2 b_2 k_r$$

$$k_{42} = k_{24} = -b_1 k_{\rm f}$$

$$k_{52} = k_{25} = b_2 k_{\rm f}$$

$$k_{33} = 2k_f a_1^2 + 2k_r a_2^2$$

$$k_{44} = k_f + k_{tf}$$

$$k_{55} = k_f + k_{tf}$$

A.2. Quarter car model

A.2.1. Quarter car model parameters

See Table A2.

Table A2
Suspension system parameters [14].

Parameters	Value	Unit
Sprung mass m _s	250	[kg]
Unsprung mass m _{us}	53	[kg]
Suspension stiffness ksq	10 ⁴	[N/m]
Tire stiffness ktq	$20\cdot 10^4$	[N/m]
Suspension damping c_{sq}	1000	[N/ms]

A.2.2. Quarter car model motion equation

The equations of motion may be written as follows for the system at hand:

$$M\ddot{X} + C\dot{X} + KX = F$$

The matrices of this system are given by:

$$[M] = \begin{bmatrix} m_s & 0 \\ 0 & m_{us} \end{bmatrix}$$

$$X = \begin{bmatrix} x_1 \\ x_2 \end{bmatrix}$$

$$[C] = \begin{bmatrix} c_{sq} & -c_{sq} \\ -c_{sq} & c_{sq} \end{bmatrix}$$

$$[K] = \begin{bmatrix} k_{sq} & -k_{sq} \\ -k_{sq} & k_{sq} + k_{tq} \end{bmatrix}$$

$$\{F\} = \left[\begin{array}{c} 0 \\ k_{tq}y \end{array} \right]$$

A.3. Half car model (Pitch model)

A.3.1. Pitch model parameters

See Table A3.

Table A3Pitch model parameters [14].

Parameters	Value	Unit
Mass of the chassis m _p	500	[kg]
Mass of the tire m _{fp}	53	[kg]
Mass of the tire m _{rp}	76	[kg]
Suspension stiffness k _{sfp}	$13 \cdot 10^{3}$	[N/m]
Suspension stiffness k _{srp}	10^{4}	[N/m]
Tire stiffness k_{tfp}/k_{trp}	$20 \cdot 10^4$	[N/m]
Suspension damping c _{sfp/} c _{srp}	1000	[N/ms]
Pitch moment of inertia Iy	550	$[kg/m^2]$
Distance of gravity centre from front axle a ₁	1.5	[m]
Distance of gravity centre from rear axle a ₂	1.57	[m]

A.3.2. Motion equations

$$M\ddot{X} + C\dot{X} + KX = F$$

with

$$X {=} \begin{bmatrix} x \\ \theta \\ x_{p1} \\ x_{p2} \end{bmatrix} \quad M {=} \begin{bmatrix} m_p & 0 & 0 & 0 \\ 0 & I_y & 0 & 0 \\ 0 & 0 & m_{f\,p} & 0 \\ 0 & 0 & 0 & m_{rp} \end{bmatrix}$$

$$\mathbf{K} = \begin{bmatrix} \mathbf{k}_{sfp} + k_{srp} & a_2 \mathbf{k}_{srp} - a_1 \mathbf{k}_{sfp} & -k_{sfp} & -k_{srp} \\ a_2 \mathbf{k}_{srp} - a_1 \mathbf{k}_{sfp} & a_1^2 \mathbf{k}_{sfp} + a_2^2 \mathbf{k}_{srp} & a_1 \mathbf{k}_{sfp} & -a_2 \mathbf{k}_{srp} \\ -k_{sfp} & a_1 \mathbf{k}_{sfp} & \mathbf{k}_{sfp} + k_{tfp} & 0 \\ -k_{srp} & -a_2 \mathbf{k}_{srp} & 0 & \mathbf{k}_{srp} + \mathbf{k}_{trp} \end{bmatrix}$$

$$\mathbf{C} = \begin{bmatrix} \mathbf{c}_{sfp} + c_{srp} & a_2\mathbf{c}_{srp} - a_1\mathbf{c}_{sfp} & -c_{sfp} & -c_{srp} \\ a_2\mathbf{c}_{srp} - a_1\mathbf{c}_{sfp} & a_1^2\mathbf{c}_{sfp} + a_2^2\mathbf{c}_{srp} & a_1\mathbf{c}_{sfp} & -a_2\mathbf{c}_{srp} \\ -c_{sfp} & a_1\mathbf{c}_{sfp} & \mathbf{c}_{sfp} & 0 \\ -c_{srp} & -a_2\mathbf{c}_{srp} & 0 & \mathbf{c}_{srp} \end{bmatrix}$$

$$F = \begin{bmatrix} 0 \\ 0 \\ k_{tfp}r_1 \\ k_{trp}r_2 \end{bmatrix}$$

A.4. Half car model (Roll model)

A.4.1. Roll model parameters

See Table A4.

Table A4
Roll model parameters [14].

Parameters	Value	Unit
Mass of the chassis m _b	500	[kg]
Mass of the tires m _{ur1}	53	[kg]
Suspension stiffness ksr1	$11.5 \cdot 10^3$	[N/m]
Tire stiffness k _{ur1}	$20 \cdot 10^4$	[N/m]
Suspension damping c_{sr1}/c_{sr2}	1000	[N/ms]
Roll moment of inertia I _x	410	$[kg/m^2]$
Distance of gravity centre from right axle b1	0.7	[m]
Distance of gravity centre from left axle b2	0.75	[m]

A.4.2. Motion equations

$$M\ddot{X} + C\dot{X} + KX = F$$

with

$$X = \begin{bmatrix} x_b \\ \varphi \\ x_{u1} \\ x_{u2} \end{bmatrix}$$

$$M {=} \begin{bmatrix} m_b & 0 & 0 & 0 \\ 0 & I_x & 0 & 0 \\ 0 & 0 & m_{ur1} & 0 \\ 0 & 0 & 0 & m_{ur2} \end{bmatrix}$$

$$\mathbf{K} = \begin{bmatrix} \mathbf{k_{sr1}} + \mathbf{k_{sr2}} & -b_2\mathbf{k_{sr2}} + b_1\mathbf{k_{sr1}} & -k_{sr1} & -k_{sr2} \\ -b_2\mathbf{k_{sr2}} + a_1\mathbf{k_{sr1}} & b_1^2\mathbf{k_{sr1}} + b_2^2\mathbf{k_{sr2}} & -b_1\mathbf{k_{sr1}} & b_2\mathbf{k_{sr2}} \\ -k_{sr1} & -b_1\mathbf{k_{sr1}} & \mathbf{k_{sr1}} + k_{ur1} & 0 \\ -k_{sr2} & -b_2\mathbf{k_{sr2}} & 0 & \mathbf{k_{sr2}} + \mathbf{k_{ur2}} \end{bmatrix}$$

$$\mathbf{C} = \begin{bmatrix} \mathbf{c_{sr1}} + \mathbf{c_{sr2}} & -b_2\mathbf{c_{sr2}} + b_1\mathbf{c_{sr1}} & -c_{sr1} & -c_{sr2} \\ -b_2\mathbf{c_{sr2}} + b_1\mathbf{c_{sr1}} & b_1^2\mathbf{c_{sr1}} + b_2^2\mathbf{c_{sr2}} & -b_1\mathbf{c_{sr1}} & b_2\mathbf{c_{sr2}} \\ -c_{sr1} & -b_1\mathbf{c_{sr1}} & \mathbf{c_{sr1}} & 0 \\ -c_{sr2} & -b_2\mathbf{c_{sr2}} & 0 & \mathbf{c_{sr2}} \end{bmatrix}$$

$$\mathbf{C} = \begin{bmatrix} \mathbf{c_{sr1}} + \mathbf{c_{sr2}} & -b_2\mathbf{c_{sr2}} + b_1\mathbf{c_{sr1}} & -c_{sr1} & -c_{sr2} \\ -b_2\mathbf{c_{sr2}} + b_1\mathbf{c_{sr1}} & b_1^2\mathbf{c_{sr1}} + b_2^2\mathbf{c_{sr2}} & -b_1\mathbf{c_{sr1}} & b_2\mathbf{c_{sr2}} \\ -c_{sr1} & -b_1\mathbf{c_{sr1}} & \mathbf{c_{sr1}} & \mathbf{0} \\ -c_{sr2} & -b_2\mathbf{c_{sr2}} & \mathbf{0} & \mathbf{c_{sr2}} \end{bmatrix}$$

$$F = \begin{bmatrix} 0 \\ 0 \\ k_{ur1}h_1 \\ k_{ur2}h_2 \end{bmatrix}$$

References

- [1] Yu W, Zhang X, Guo K, Karimi HR, Ma F, Zheng F. Adaptive real-time estimation on road disturbances properties considering load variation via vehicle vertical dynamics. Math Problems Eng 2013;2013. http://dx.doi.org/10.1155/2013/283528. 9 pages, Article ID 283528.
- [2] Hasbullah F, Faris WF, Darsivan FJ, Abdelrahman M. Ride comfort performance of a vehicle using active suspension system with active disturbance rejection control. Int J Veh Noise Vib 2015;11(1):78-101.
- [3] Fauriat W, Mattrand C, Gayton N, Beakou A, Cembrzynski T. Estimation of road profile variability from measured vehicle responses. Veh Syst Dyn 2016:54(5):585-605
- [4] Sayers MW, Gillespie TD, Queiroz AV. The international road roughness experiment. Establishing correlation and a calibration standard for measurements (No. HS-039 586): 1986.
- Gillespie TD, Sayers MW, Segel L. Calibration of response-type road roughness measuring systems. NCHRP Report, vol. 228; 1980.
- [6] Harris NK, González A, OBrien EJ, McGetrick P. Characterisation of pavement profile heights using accelerometer readings and a combinatorial optimisation technique. J Sound Vib 2010;329(5):497-508.
- Doumiati M, Victorino A, Charara A, Lechner D. Estimation of road profile for vehicle dynamics motion: experimental validation. San Francisco, CA: IEEE American

- Control Conference (ACC); 2011. p. 5237-5242.
- Akrout A, Tounsi D, Taktak M, Abbès MS, Haddar M. Estimation of dynamic system's excitation forces by the independent component analysis. Int J Appl Mech 2012:4(03):1250032
- Hassen DB, Miladi M, Abbes MS, Baslamisli SC, Chaari F, Haddar M. Application of the operational modal analysis using the independent component analysis for a quarter car vehicle model. In Advances in Acoustics and Vibration. Springer International Publishing; 2017. p. 125–33.
- [10] Hyvärinen A, Oja E. Independent component analysis: algorithms and applications. Neur Networks 2000;13(4):411-30.
- Jutten C, Herault J. Blind separation of sources, Part I: An adaptive algorithm based on neuromimetic architecture. Signal Process 1991;24(1):1-10.
- Comon P. Independent component analysis, a new concept? Signal Process 1994;36(3):287-314.
- [13] Zarzoso V, Comon P. Robust independent component analysis by iterative maximization of the kurtosis contrast with algebraic optimal step size. IEEE Trans Neural Networks 2010;21(2):248-61.
- Jazar RN. Vehicle dynamics: theory and application. Springer Science & Business Media; 2013.
- Abbes MS, Chaabane MM, Akrout A, Fakhfakh T, Haddar M. Vibratory behavior of a double panel system by the operational modal analysis. Int J Model, Simul, Sci Comput 2011;2(04):459-79.